AUTONOMOUS AND TETHERED DRONE-BASED LORA MESH NETWORK SYSTEM FOR UNINTERRUPTED COMMUNICATION IN DISASTER SITUATIONS

Çise Gül ÇAKIL

Undergraduate Student, Ankara Yıldırım Beyazıt University, Department of Aerospace Engineering

Ahmet Mert ÇETİNER

Undergraduate Student, Ankara Yıldırım Beyazıt University, Department of Aerospace Engineering

Muhammet Esat HACIKERİMOĞLU

Undergraduate Student, Ankara Yıldırım Beyazıt University, Department of Aerospace Engineering

ABSTRACT

The resilience of societies against disasters relies on the uninterrupted operation of critical infrastructures such as communication, energy, and transportation. However, the rapid collapse of existing terrestrial infrastructures during large-scale disasters like earthquakes and floods disrupts the coordination of search-and-rescue operations and directly reduces response effectiveness. In this context, infrastructure-independent, rapidly deployable, and autonomous Unmanned Aerial Vehicle (UAV) based communication systems emerge as a strategic solution. A review of the literature reveals that coverage optimization, energy continuity, and network capacity issues are mostly addressed independently. In particular, the "first-mile" access problem—stemming from signal attenuation when victims attempt to connect directly to capacity-limited aerial platforms—and the battery limitations of free-flying UAVs constitute significant research gaps.

This study proposes a multidisciplinary, integrated, and scalable system architecture to overcome these bottlenecks in the literature. The proposed model is a decoupled "Dock-Tether-Drone" architecture comprising an autonomous ground station (dock) integrated into street infrastructure (light poles), a tethered UAV platform, and a LoRa-based mesh network. By enabling disaster victims to connect to ground-level stations via Wi-Fi instead of directly to aerial vehicles, the access problem is resolved at the hardware level. The collected data is seamlessly transferred via a composite/fiber-optic cable, which concurrently provides continuous power to the UAV. Furthermore, to prevent data bottlenecks (sinkholes) during large-scale disasters, a hierarchical (two-tier) network structure is designed. In this framework, local tethered UAV networks at the street level offload communication to high-altitude strategic UAVs (e.g., AKSUNGUR) when data traffic peaks.In conclusion, by eliminating battery and hardware access constraints, this innovative architecture offers a rapidly deployable and highly resilient communication infrastructure, enabling uninterrupted communication between disaster victims and search-and-rescue teams.

Keywords: Disaster Communication, Tethered UAV, LoRa Mesh Network, Two-Tier Network Architecture, Uninterrupted Communication

1. INTRODUCTION

The continuity of modern societies depends on the uninterrupted functioning of critical infrastructure systems — communication, energy, and transportation in particular. Earthquakes, floods, and similar disasters can render these systems inoperable within hours, disrupting the flow of information that underpins effective disaster management. When terrestrial base stations go offline, fiber-optic lines are severed, and power grids collapse, search-and-rescue coordination becomes significantly harder and response effectiveness drops directly.

The first hours after a disaster are decisive. Continuous communication is vital both for coordinating teams and for guiding survivors toward safe areas. Because existing infrastructure cannot be restored quickly enough in the aftermath, communication blackouts become nearly inevitable. Unmanned Aerial Vehicle (UAV)-based systems have emerged as a promising response to this problem. Aerial base stations (ABS) and flying ad-hoc networks (FANET) can provide rapid coverage over wide areas thanks to their mobility and line-of-sight (LoS) propagation characteristics. Sustaining these systems in real field conditions, though, requires more than maximizing coverage; user access, energy continuity, and network capacity must be addressed together.

1.1 Literature Review

UAV-based communication systems in the literature are examined along three main axes: coverage and 3D positioning, energy management and platform architecture, and communication technologies and network structures:

Coverage & 3D Positioning

The use of UAVs as Aerial Base Stations (ABS) gives rise to the problem of optimal placement in three-dimensional space. Models based on Mixed Integer Linear Programming (MILP) offer strategies for maximizing user coverage with a minimum number of UAVs [1]. Al-Hourani et al. [2] demonstrated, through a probabilistic line-of-sight model, that the optimal altitude varies depending on the density of the surrounding built environment. Experimental studies support this approach: McRae et al. [3] showed that a UAV relay positioned at approximately 122 m altitude can overcome line-of-sight obstacles and maintain communication continuity.

Coverage performance is also directly affected by signal parameters. In LoRa-based systems, spreading factor and bandwidth play a decisive role in range and must be evaluated in conjunction with altitude selection [4]. The non-uniform distribution of users creates a need for more realistic models in coverage planning. In this context, population density–based heat maps stand out as an approach that improves resource allocation accuracy and placement precision [5].

Energy Management

Free-flying UAVs have limited flight times due to lithium-based battery technologies [6], which makes the sustainability of long-duration missions challenging. Both software and hardware solutions have been developed in the literature to overcome these limitations. Qiu et al. [7] proposed dynamic trajectory models that minimize energy consumption using deep reinforcement learning–based algorithms. However, even such algorithmic improvements cannot extend operational time beyond the energy density limitations of batteries. Zeng and Zhang [8] showed that energy consumption depends not only on mission planning but also on

aerodynamic parameters such as flight speed, altitude, and flight type, demonstrating that energy optimization is a multi-variable problem.

Among hardware solutions, tethered UAV systems stand out. These systems enable long-duration missions by providing continuous energy delivery from a ground station [9, 10]. However, cable weight and aerodynamic effects limit performance. To mitigate these constraints, the industry has implemented high-voltage DC transmission techniques to minimize energy transmission losses, along with mechanical design improvements aimed at increasing cable stability under wind loading.

Communication Technology

The failure of conventional communication infrastructure during disasters brings alternative technologies to the fore. In this context, LoRa-based systems stand out for their low power consumption and long-range capabilities [11, 12]. LoRa modulation can provide reliable data transmission even at low signal-to-noise ratios. Studies on UAV-assisted LoRa networks show that aerial coverage enhances communication performance [13].

The practical applicability of LoRa-based mesh architectures for infrastructure-independent communication has been field-validated through the open-source Meshtastic project. Built on standard LoRa hardware, Meshtastic operates on a flooding-based, self-healing mesh protocol with more than 40,000 active nodes worldwide, providing a concrete reference model for disaster and remote-area communication [14].

Mesh network architectures offer flexible and resilient systems without relying on centralized infrastructure [15, 16]. However, LoRa systems' low data rate and duty cycle constraints limit capacity. To overcome these limitations, NOMA-based access techniques, multi-channel management, and frequency sharing strategies have been proposed [17].

Real Disaster Applications

Real disaster scenarios directly reveal system performance beyond theoretical models. According to media reports, the "Dronecell" concept developed in Turkey — with a flight time of approximately 30–35 minutes — was unable to provide a sustainable solution in the face of widespread destruction and power outages during the February 6, 2023 Kahramanmaraş earthquakes [18]. The large-scale failure of terrestrial base stations during the disaster made the need for aerial platforms evident. In this context, it has been reported in media sources that the AKSUNGUR UAV developed by TUSAŞ provided mobile communication by flying over Hatay for hours [19]. This operation demonstrates the field applicability of the aerial base station concept. However, the runway dependency and limited deployment flexibility of large platforms highlight the need for systems that can be rapidly deployed at a local scale.

1.2 Literature Gap

In conclusion, the literature clearly demonstrates that UAV-based communication systems hold significant potential in disaster scenarios. Nevertheless, a substantial portion of existing studies address coverage, energy, and spectrum problems in isolation, without evaluating these parameters within an integrated optimization framework. In particular, the simultaneous treatment of capacity limitations in LoRa-based systems, the spatial clustering of user density, and energy continuity problems remains a significant research gap in the literature.

Chief among these deficiencies is the "first-mile" problem, which defines how users access the system. The majority of existing studies assume that users can connect directly to UAVs; however, it is well established in practice that this approach is not sustainable due to electromagnetic noise, device power limitations, and signal attenuation [13, 20]. This constitutes a critical gap that directly affects system performance yet receives limited attention in the literature.

The second significant deficiency concerns the modeling of user distribution. The great majority of existing optimization studies rely on the assumption that users are homogeneously distributed. In real disaster scenarios, however, individuals cluster in specific areas, placing a considerable burden on network capacity. In systems with low data rates such as LoRa, this concentration can lead to data collisions and spectral congestion problems [11, 12]. The scarcity of studies that directly integrate user density into the optimization model indicates that this is an important research gap.

Third, there are also notable deficiencies in the areas of energy continuity and hardware integration. The battery limitations of free-flying UAVs constrain long-duration operations, and while tethered systems do provide continuous energy, existing solutions are generally based on large-scale platforms with low portability [10]. Furthermore, the literature contains an insufficient number of studies on the integration of ground station designs into urban infrastructure. Although existing patent solutions offer innovative approaches, the lack of compact, modular systems suitable for intra-urban applications is conspicuous.

Finally, it is evident from the literature that coverage, energy, and communication capacity problems are most often treated independently of one another. In a real disaster scenario, however, these parameters are strongly coupled, and optimizing them separately limits overall system performance [17]. This clearly underscores the need for interdisciplinary and integrated system architectures. Moreover, the high computational cost of the 3D positioning optimization models found in the literature [1] limits their applicability in real-time disaster response scenarios.

1.3 Novelty

A review of the literature reveals that none of the existing works simultaneously address the following three characteristics. First, the integration of tethered UAV infrastructure with a LoRa mesh network within a single architectural framework: tethered system studies [9, 10] focus on energy continuity while not addressing communication protocol design, whereas LoRa network studies [11, 12, 13] treat the energy infrastructure as a given, assuming either free-flying UAVs or fixed stations. Second, regarding the first-mile problem: the great majority of existing works [1, 2] assume that users can connect directly to the aerial platform, yet it is documented that this assumption is invalidated in practice by electromagnetic noise and limited antenna power [20]. In the proposed architecture, this problem is resolved at the hardware level through a ground-level Wi-Fi access point, enabling standard user devices to access the system without requiring any software modification. Third, energy continuity and network capacity optimization are not addressed jointly: these two problems are modeled independently in the literature [17], and this separation limits system performance under real disaster conditions. The DTD architecture closes all three of these gaps within a single integrated design framework, by virtue of its functional decomposition principle.

The original contributions of the proposed system are presented below under four main headings:

Hardware-Level First-Mile Solution

Rather than having users connect directly to the UAV, access is provided through autonomous dock stations at ground level via Wi-Fi, thereby eliminating high path loss and low SNR problems at the hardware level [13].

Simplified 1D Altitude Optimization Based on Real User Density

By fixing dock stations to urban infrastructure, the 3D positioning problem is reduced to a one-dimensional altitude optimization with low computational cost. The model jointly addresses user density and LoRa capacity constraints [2].

Two-Tier Hierarchical Mesh Architecture to Prevent Sinkhole Problem

When data traffic intensifies, dynamic load transfer from local tethered UAV networks to high-altitude platforms prevents the sinkhole (traffic bottleneck) problem.

Component-Level Autonomous, Urban-Integrated Design with Tethered Energy Supply

The tethered structure provides uninterrupted energy while interference-free data transmission is achieved via fiber-optic line, eliminating battery constraints and enhancing system continuity [9, 10].

1.4 Conceptual Framework: Design Logic of the DTD Architecture

Articulating the design logic of the proposed system architecture at a conceptual level is essential for justifying methodological decisions and connecting them to the literature gaps identified above. This section presents the system's core design philosophy, the direct mapping between research gaps and design decisions, the system hierarchy, and the assumptions that apply throughout the methodology.

1.4.1 Core Design Philosophy: Functional Decomposition

The primary constraint of existing UAV-based communication systems is the tendency to integrate energy generation and data transmission within a single aerial platform. This coupling means that the limitations of each function directly constrain all others — battery capacity simultaneously limits flight duration, network capacity, and access quality. The DTD architecture breaks this constraint through functional decomposition, assigning each function to a separate physical layer that can be independently optimized:

- Energy function → continuous delivery via tether cable from the ground station (dock)
- User access function → ground-level Wi-Fi access point
- Data transmission function → airborne LoRa mesh network and fiber-optic backhaul

With this separation, a constraint in any one layer no longer propagates directly to the others. If battery power runs out, the network does not collapse; if LoRa capacity fills up, user access is not cut off — instead, the relevant layer is independently scaled or traffic is offloaded to the next tier.

1.4.2 Research Gap–Design Decision Mapping

The four research gaps identified in Section 1.2 are directly mapped to DTD design decisions, one-to-one. This mapping demonstrates that the proposed architecture is a systematic engineering response to specific deficiencies in the literature.

Table 1. Research gaps and corresponding DTD design decisions

Research Gap	DTD Design Decision	Implementing Component
Battery constraint: 25–35 min operational limit of free-flying UAVs	Tethered power line: continuous HVDC delivery from ground station	Hybrid composite cable + TMS
First-mile access problem: connection attempts to UAV fail due to signal attenuation	Ground-level Wi-Fi access point: reduces user-platform distance to zero	Dock station, IEEE 802.11n
Sinkhole bottleneck: traffic congestion near gateway in centralized mesh architectures	Two-tier hierarchical mesh: offloading to upper platform when capacity is exceeded	Layer 2 → Layer 3 offload
Homogeneous user distribution assumption: existing models do not reflect real disaster clustering	GMM-based population model and Weighted K-Means dock placement	WorldPop/CDR data integration
High computational cost of 3D positioning optimization	Fix dock horizontal position; reduce problem to 1D altitude assignment	Micro-optimization model

1.4.3 System Hierarchy and Inter-Layer Interaction

The DTD architecture consists of three operational layers, each independently functional but connected through well-defined interfaces. Figure 1 summarizes this hierarchical structure and the energy, data, and traffic flows between layers.

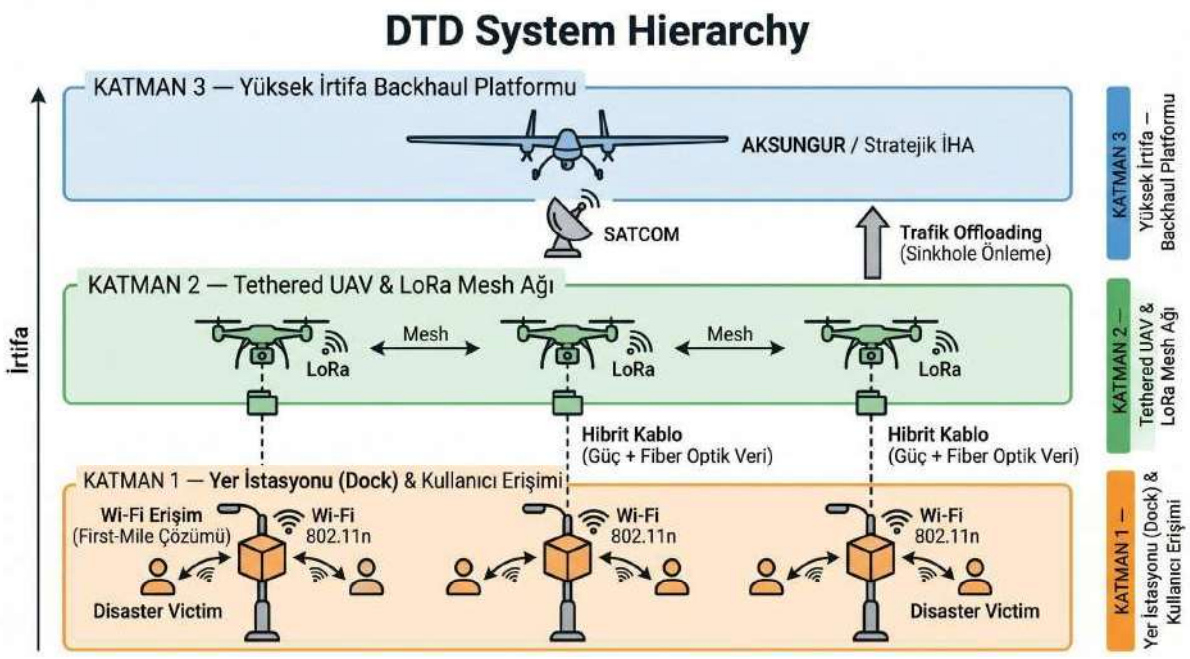

Figure 1. DTD System Hierarchy: Functional representation of operational layers and inter-layer energy, data, and traffic flow interfaces.

Layer 1 (Ground Station) is the system's ground-level access and energy layer. Disaster victims and field teams connect to this layer via standard Wi-Fi. User data is collected here and

forwarded to Layer 2 through the fiber-optic channel inside the hybrid tether cable; simultaneously, the cable delivers continuous power to the Layer 2 UAV.

Layer 2 (Tethered UAV and LoRa Mesh) is the local communication and aerial platform layer. Each tethered UAV manages LoRa mesh nodes within its coverage area and optimizes inter-node routing through the ECHO protocol. When local network capacity approaches its threshold, traffic is offloaded to Layer 3.

Layer 3 (High-Altitude Backhaul) is the long-range backbone communication layer. Strategic UAV platforms receive excess traffic from Layer 2 networks and distribute it across large geographic areas; SATCOM integration provides ground-independent backhaul connectivity.

Inter-layer interaction occurs through three interfaces: a physical hybrid cable (power + fiber-optic data) between Layers 1 and 2; RF-based LoRa mesh within Layer 2; and an RF/SATCOM-based offloading link between Layers 2 and 3.

1.4.4 Design Constraints and Methodological Assumptions

The following assumptions apply throughout the conceptual and analytical evaluation of the proposed architecture. They preserve analytical tractability while adequately representing realistic disaster scenarios.

Platform dynamics: The UAV is assumed to hover at a fixed altitude. Position deviations due to wind perturbations are considered negligible, as TMS active tension control maintains stability.

Atmospheric conditions: Wind speed is assumed to be uniformly distributed in the horizontal plane and invariant with altitude. Incorporating real atmospheric profiles is left for future work.

LoRa network traffic: Mesh nodes are assumed to generate data at a fixed rate, with traffic intensity changing gradually over time. Sudden load increases are absorbed by the two-tier offloading mechanism.

User distribution: The spatial user density in the disaster area is assumed to be adequately represented by a Gaussian Mixture Model (GMM). WorldPop and CDR data are assumed to reflect post-disaster population movement in near real time.

Scope: Simulation environments and physical prototype construction are outside the scope of this work. The methodology provides a conceptual, mathematical, and analytical design validation; field-experimental verification is identified as a primary research objective for future studies.

2. METHODOLOGY

2.1 Methodological Workflow

The analysis of the proposed DTD architecture follows a systematic, multi-stage methodology. The fundamental approach is to decompose the complex, multidisciplinary system into modular subsystems, model each subsystem analytically, and construct a coherent design chain linking their outputs. This work does not present experimental validation; instead, it offers a design-oriented analytical framework grounded in models that have been validated in field or simulation studies. Every equation used is traceable to such sources.

The methodological process comprises six sequential stages — not independent modules, but a linear design chain in which each stage's output becomes the next stage's input constraint.

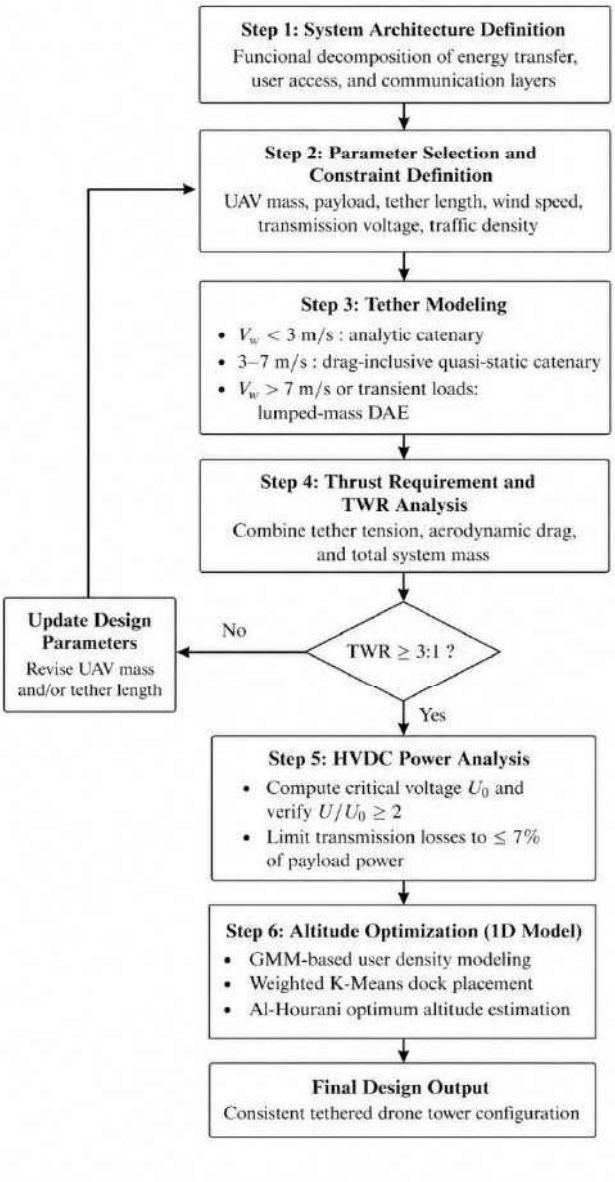

Figure 2. Design and analysis methodology of the tethered UAV system.

In essence: cable mass and aerodynamic load are first computed using a drag model; tension and thrust analysis follow; the TWR constraint is checked; and finally energy and altitude optimization are performed. System-level consistency emerges naturally from this chain structure.

Table 2. DTD architecture design parameters, nominal ranges, and selection rationale

Parameter	Symbol	Nominal Range	Selection Rationale	Source
UAV mass	m_drone	8–12 kg	Commercial hexarotor class satisfying TWR ≥ 3	[9, 10]
Payload mass	m_payload	2–5 kg	LoRa module + antenna array + mission computer	[9]
Cable length	l	50–150 m	Lower bound: LoS angle constraint; upper bound: TWR margin critical threshold due to drag and cable mass increase	[9, 10]
Cable unit mass	ρ_cable	0.08–0.15 kg/m	Typical hybrid composite Kevlar/copper/fiber cable class	[9, 10]
Wind speed	V_w	0–10 m/s	Multirotor operational stability threshold; above this, VRS risk increases	[9]
HVDC voltage	U	48–100 V	Lower bound: critical voltage threshold U_0; upper bound: standard DC component safety class	[24]
LoRa spreading factor	SF	7–12	SF9 nominal; lower SF favors speed, higher SF favors range/reliability	[11, 12]
Bandwidth	BW	125 kHz / 500 kHz	125 kHz: frequency diversity across channels; 500 kHz: single-channel high-throughput mode	[11]

2.2 System Architecture: The Dock–Tether–Drone Framework

The proposed DTD architecture rests on a three-layer system structure that physically separates energy delivery, user access, and data communication. This is a direct implementation of the functional decomposition principle introduced in Section 1.4.

2.2.1 Layer 1 – Ground Station (Dock) and User Access

The ground station (dock) forms the system's energy and user access layer. It combines autonomous UAV landing and takeoff management, a continuous power supply, and a user access point within a single physical unit. Compact and modular in design, the dock can be pre-deployed at urban reference points such as schools, parks, or municipal buildings — enabling rapid activation without human intervention at the moment of a disaster. The enclosure meets IP65 protection standards, ensuring operational continuity against dust, moisture, and rain.

User Access Layer — First-Mile Solution

Disaster victims and field teams connect to the dock via an IEEE 802.11n Wi-Fi access point using standard smartphones or portable devices. Selecting 802.11n is a deliberate engineering decision: operating in the 2.4 GHz band, this standard offers a larger coverage radius (200–250 m in open areas), better penetration through debris, and broader device compatibility compared to 802.11ac's 5 GHz band. The 802.11ac mode is positioned as a secondary layer for capacity reinforcement under higher user densities.

Al-Hourani et al. [2] showed, through a probabilistic path loss model for low-altitude aerial platforms, that high path losses make direct user-to-UAV connections unreliable at ground level. Darwajkar et al. [20] experimentally documented that electromagnetic noise and the limited antenna power of end devices render this approach impractical in the field. The proposed architecture addresses this at the hardware level: user data is collected at ground level and forwarded to the UAV through the fiber-optic data channel inside the tether cable.

Table 3. UAV Direct Connection vs. Dock (Ground Wi-Fi) Comparison [2, 20]

Parameter	UAV Direct Connection	Dock (Ground Wi-Fi)
Distance	80–150 m (air-to-ground)	0–50 m
Path Loss Model	Air-to-Ground (high loss)	Indoor/Urban (lower loss)
Average Path Loss	~110–130 dB	~60–80 dB
SNR	Low (0–10 dB)	High (20–40 dB)
Connection Reliability	Low	High
Device Power Requirement	High	Low

This comparison quantitatively establishes that direct UAV connection is not practically sustainable in disaster environments, and that the proposed dock-based approach offers an SNR advantage of approximately 40–50 dB.

Power Management System and Backup Architecture

The dock's power management unit integrates grid power, a backup diesel generator, and solar panels within a smart distribution architecture that switches automatically to backup when grid power is lost. Energy delivered to the UAV travels as high-voltage DC; onboard DC-DC converters step it down to the levels required by the motors and avionics. Fattori and Cocuzza [9] highlight the need for a backup battery system connected in parallel to the DC bus — typically comprising pre-charged batteries, solid-state relays (SSR), and fast-switching diodes — that engages automatically upon voltage drop detection. This circuit allows the UAV to initiate a safe landing procedure via the MAVLink Failsafe protocol in the event of cable failure or grid loss.

Tether Management System (TMS)

The TMS is the most critical mechatronic component of the DTD architecture, managing cable tension and length in real time. Fattori and Cocuzza [9] define its primary functions as storing and dispensing excess cable, sensing and controlling cable parameters (length, tension, angle), and optionally housing the power source. Active tension control operates through three mechanisms: load cells detect sudden wind loads and trigger rapid cable release to dampen impulse shock on the UAV; the cable is retracted at high speed (≥2 m/s) during UAV descent to prevent propeller entanglement; and when GNSS is unavailable in disaster environments, fuzzy logic algorithms estimate UAV position from cable angle and tension changes to maintain stability.

Telemetry exchange between the UAV flight controller and TMS runs over the MAVLink protocol. Specialized dialect messages include TETHER_ATTACH_STATUS (#11035) for reporting real-time tension-voltage-current telemetry and TETHER_CONTROL (#11036) for transmitting Lock Cable / Increase Tension / Emergency Release commands. Any power interruption or cable break triggers the Failsafe protocol, which transitions the UAV to battery mode and initiates a safe landing procedure [9].

Safety Mechanisms

Safe operation is monitored through three hierarchically interacting priorities. First, cable tension is kept below the breaking strength (≈98 N for a Kevlar core); if this limit is exceeded, the TMS automatically releases the cable. Second, cable elongation is held below 0.5% to protect the integrated optical fibers — achievable with high tensile-strength materials such as Kevlar. Third, the UAV's vibration velocity must not exceed the operational limits of its onboard equipment [21].

2.2.2 Layer 2 – Tethered UAV and LoRa Mesh Network

The second layer consists of a UAV physically connected to the ground station through a hybrid cable and maintained at a designated altitude in a static hover. The tethered architecture fundamentally overcomes the 25–35 minute operational ceiling of free-flying UAVs: continuous energy from the ground station means that airborne duration is theoretically limited only by the ground-based energy source. Designing a tethered system, however, is not simply an energy transfer problem — it requires simultaneous optimization of cable aerodynamics, power transmission efficiency, and the communication infrastructure.

UAV Body Configuration

Fattori and Cocuzza [9] report that, among multirotor configurations for tethered UAV systems, the hexarotor offers payload capacity up to 30 kg and multiple-motor fault tolerance, making it more reliable for disaster scenarios. Given that the DTD architecture requires the UAV to carry a LoRa module, antenna array, and mission computer, the hexarotor is the preferred platform; the final selection is determined by the thrust margin analysis in the altitude optimization stage.

2.2.2.1 Hybrid Tether Cable: Structure and Functional Role

The tether cable is a hybrid structure with four core layers: silver-plated copper conductors for power transmission, G.657A2 single-mode fiber-optic line for data, a Kevlar core for mechanical strength, and a fluoropolymer outer sheath for protection [9]. Together, these layers allow the system to simultaneously deliver continuous power to the UAV, transmit data free from electromagnetic interference, and carry mechanical loads safely.

Table 4. Hybrid tether cable layer structure and technical parameters [9]

Cable Layer	Material	Technical Advantage	Parameter
Data channel	G.657A2 single-mode fiber	Bend resistance, EMI immunity	≤0.21 dB/km @ 1550 nm; min. 7.5 mm bend radius
Power conductor	Silver-plated stranded copper	Low resistivity + light weight	6–10 A capacity
Strength member	Kevlar (Aramid)	High tensile strength	>100 kgf; 3.4 mm diameter, 1.55 kg/100 m
Outer sheath	PFA / LSZH fluoropolymer	Thermal and chemical resistance	−55°C to +200°C

Selecting the G.657A2 bend-insensitive fiber prevents signal loss caused by small-radius winding on the TMS drum during autonomous landing and takeoff cycles. Full immunity of

the fiber-optic channel to RF interference is a critical reliability advantage in the chaotic electromagnetic environment of disaster zones, ensuring stable LoRa network operation [9].

2.2.2.2 Cable Mass, Aerodynamic Behavior, and System Impact

Cable mass increases linearly with length and directly limits the UAV's operational altitude through its effect on total system weight:

$$m_{tether} = \rho_{cable} \cdot l \quad \ldots (1)$$

Fattori and Cocuzza [9] report ρ_{cable} = 0.08–0.15 kg/m for typical hybrid tether cables. The system-level consequence of this linear relationship is significant: as cable length increases, total thrust requirement rises and maximum operational altitude is constrained. This creates a direct trade-off between communication coverage and aerodynamic feasibility — higher altitude expands LoRa coverage, while longer cable increases system weight and energy consumption. Tether length is therefore not merely a mechanical parameter; it is a critical design variable that shapes communication performance.

Under wind loading, the cable is subject to aerodynamic drag forces that generate additional lateral and vertical load components on the UAV. Cable behavior in this study is represented using two models depending on operational wind conditions [22, 23]:

- **$V_w < 3$ m/s:** Analytic catenary model; static assumption is valid, solution time < 1 ms, ideal for real-time control algorithms.
- **$3 \leq V_w \leq 7$ m/s:** Drag-inclusive quasi-static catenary; aerodynamic load increases but the semi-static assumption holds.
- **$V_w > 7$ m/s:** Lumped-mass DAE model; cable segments exhibit different velocities and the static assumption loses physical fidelity; solution time ~5 ms enables integration with real-time TMS control.

In the quasi-static catenary model, cable geometry is described by:

$$y(x) = a \cdot \cosh((x - x_0)/a) + y_0 \quad \ldots (2)$$

In the lumped-mass model, aerodynamic drag force on each cable segment is:

$$F_{D,i} = (1/2) \cdot \rho \cdot A_i \cdot C_D \cdot |V_{rel,i}| \cdot V_{rel,i}, \; C_D \approx 1.0–1.2 \quad \ldots (3)$$

This modeling approach maintains a computational cost compatible with real-time control systems while providing sufficient physical accuracy[21, 22].

2.2.2.3 HVDC Power Transmission and the Energy–Altitude Link

A high-voltage direct current (HVDC) transmission strategy is employed to minimize energy transmission losses in the tether cable. This approach enables power transfer at lower current levels, thereby reducing Joule losses and allowing for a smaller cable cross-sectional area. The total power balance on the cable is formulated as [24]:

$$P_{tot} = U \cdot i = P_0 + i^2R \quad \ldots (4)$$

For real solutions to exist for current i in this equation, the supply voltage must exceed a threshold known as the critical voltage U_0:

$$U_0 = 2\sqrt{(R \cdot P_0)} \quad \ldots (5)$$

At an operating ratio of $U/U_0 = 2.0$, total transmission losses fall to just 7% of the payload power [24]. The system implication is clear: HVDC allows for thinner conductors, reducing cable mass, which in turn lowers the UAV's total thrust requirement and makes higher

operational altitudes achievable. The relationship that the minimum power requirement scales directly with drone mass [24]:

$$P_tot^{min} = (\gamma \cdot m \cdot g) / (1 - U_{\infty}/U) \quad ... (6)$$

analytically confirms that minimizing cable mass is decisive not only aerodynamically but also for energy efficiency.

2.2.2.4. Thrust Balance and TWR Analysis

In tethered UAV systems, total thrust requirement encompasses not only drone mass, payload, and cable mass, but also the vertical component of aerodynamic drag on the cable [9, 24]:

$$F_thrust = (m_drone + m_payload + m_tether) \cdot g + T_vertical + F_D,cable_vertical \quad ...(7)$$

$$TWR = F_thrust / (m_total \cdot g) \quad ...(8)$$

Here, (T_{vertical}) represents the vertical component of the cable tension, while (F_{D,cable_vertical}) denotes the vertical projection of the aerodynamic drag acting on the cable. This condition necessitates that the drone's motor–propeller combination possesses sufficient "thrust headroom" to perform agile maneuvers even when the cable reaches extreme lengths of 100–300 meters. In conventional multirotor design, it is generally required that the thrust-to-weight ratio (TWR) be at least 2:1 for stable hover, meaning that the hover condition occurs at approximately 50% throttle. However, in TUAV systems, a larger margin is required in order to counteract the downward tension generated by the cable and the lateral loads induced by wind. Fattori and Cocuzza recommend designing the TWR to be 3:1 or higher for open-area disaster response scenarios [9]. Table 2.3 summarizes TWR values for different operational conditions. Fattori and Cocuzza [9] also report that propeller interference can reduce thrust efficiency by 15–20%, and that Vortex Ring State (VRS)-like conditions at angles of attack exceeding 15° can increase power consumption by up to 60%. When these two risk factors are considered together, the design criterion of TWR ≥ 3:1 emerges for disaster response scenarios. If this criterion is not satisfied, the design cycle returns to Stage 2, where updates are made to parameters such as cable length or UAV mass [25].

Table 5. Thrust-to-weight ratio design criteria by flight scenario [9]

Flight Scenario	TWR	Aerodynamic Risk	Design Rationale
Indoor / low wind	2.0:1	Low	Basic stability margin
Industrial inspection (open area)	2.5:1	Medium — cable oscillation	Cable drag effect included
Disaster response / strong wind	≥3.0:1	High — VRS + turbulence	Propeller interference (15–20% loss) + VRS (60% power increase) safety margin

Cable Length–Coverage Trade-off

Socol's optimal cross-section analysis mathematically confirms that cable mass scales proportionally with drone mass for a given voltage and position [24]. This is consistent with Fattori and Cocuzza's experimental observations: as cable mass increases, payload capacity decreases proportionally and altitude limits are pushed [9]. The 80–150 m altitude range specified in the DTD architecture sits within the region where the cable mass–payload trade-off remains manageable and the LoRa module and mission computer can still be carried [26].

2.2.2.5 Tether Management System (TMS)

The TMS manages cable tension and length in real time. Fattori and Cocuzza [9] define its primary functions as storing and dispensing excess cable, sensing and controlling cable parameters, and optionally housing the power supply. Active tension control is achieved through three mechanisms: load cells detect sudden wind loads and trigger rapid cable release to dampen impulse shock on the UAV; the cable is retracted at high speed during descent to prevent propeller entanglement; and fuzzy logic algorithms estimate UAV position from cable angle and tension changes when GNSS is unavailable. Telemetry exchange with the flight controller runs over MAVLink; cable failure or power loss triggers the Failsafe protocol and initiates a safe landing [27, 28].

2.1.2.6 LoRa Technology: Selection Rationale and Key Characteristics

LoRa (Long Range) is a low-power wireless communication technology based on Chirp Spread Spectrum (CSS) modulation, operating in the unlicensed ISM band [11, 12]. LoRa modulation operates at SNR thresholds ranging from –7.5 dB to –20 dB depending on the spreading factor (SF7: –7.5 dB, SF12: –20 dB); at the default SF9 configuration, reliable data transmission is achieved at a threshold of –12.5 dB [11, 12]. The primary rationales for selecting LoRa in the context of disaster communication are as follows: fully infrastructure-independent operation (requiring neither GSM nor fiber lines); a range capacity exceeding 2–5 km in urban environments and 15 km in open areas [29]; unlicensed ISM band operation in Turkey; and power consumption of approximately 28 mA in transmission mode, 10 mA in reception mode, and 0.2 µA in sleep mode [30] — yielding an average current consumption of less than 11 mA under a 1% duty cycle condition. When compared to the typical consumption of 150–800 mA for Wi-Fi and 200–500 mA for LTE modems, LoRa's energy advantage is clearly evident. Table X summarizes the critical parameters of LoRa, Wi-Fi, LTE, and Zigbee technologies from a disaster scenario perspective.

Table 6. Communication technology comparison for disaster scenarios

Feature	LoRa/LoRaWAN	Wi-Fi (802.11)	LTE/5G	Zigbee
Range (open area)	2–15 km	50–100 m	1–10 km (BTS-dependent)	10–100 m
Power consumption	Very low (mA)	Medium–High	High	Low
Infrastructure dependency	None (mesh)	Medium	High (BTS)	Medium
Data rate	0.3–22 kbps (868 MHz)	Mbps–Gbps	Mbps–Gbps	20–250 kbps
Penetration capability	High	Low	OMedium	Medium
Disaster scenario suitability	Very High	Low	Requires BTS	Limited range
License requirement	None (ISM)	None	Yes	None
Mesh support	Yes (LoRa Mesh)	Limited	No	Yes

Beyond these rationales, the Meshtastic open-source project provides an experimental basis for LoRa's practical applicability in disaster communication. Meshtastic combines low hardware cost, firmware-level self-healing mesh, and application-level encrypted communication within a single stack [31]. The proposed DTD architecture scales this proven mesh logic by integrating it into a tethered UAV infrastructure, while structurally eliminating the energy continuity constraint.

Unlike the classic LoRaWAN star topology — which is dependent on a central gateway — the proposed architecture adopts a mesh topology that removes this dependency [15, 16]. In a mesh structure, each node acts as both an end device and a router; when a node goes offline or moves out of coverage, data traffic is automatically rerouted through alternative paths. This self-healing capability directly enhances network resilience against the unpredictable dynamics of disaster environments.

2.1.2.7 Frequency Band and Channel Architecture

The proposed system operates in the 868 MHz ISM band. The rationale for this choice is multi-dimensional: unlicensed use in Turkey and Europe, lower free-space path loss compared to 2.4 GHz, and superior penetration through urban structures. The 868 MHz band is subdivided into sub-channels under the ETSI EN 300 220 standard; the proposed architecture uses three primary channels at 868.1 MHz, 868.3 MHz, and 868.5 MHz, and frequency diversity is achieved through this multi-channel structure [11]. In the multi-channel configuration, each channel operates at a bandwidth of 125 kHz; under high-traffic conditions, a switchover to 500 kHz BW on a single channel is performed. The 500 kHz BW mode is applied only in single-channel operation; multi-channel frequency diversity is achieved with the 125 kHz BW configuration. This structure significantly reduces the congestion and collision problems to which single-channel systems are susceptible [17].

The proposed architecture is built upon two complementary spectrum layers within the scope of ETSI EN 300 220. In the first layer, routine beacon traffic — such as periodic position reporting and status updates — is carried over the g1 sub-band (868.0–868.6 MHz, 1% duty cycle, 25 mW). For a typical 20-byte beacon packet, the Time-on-Air (ToA) value is 61.70 ms; with one transmission per minute, duty cycle utilization remains at only 0.1%, meaning the 1% budget is sufficient for routine operation. In the second layer, the g3 sub-band (869.4–869.65 MHz) is activated for time-sensitive traffic such as high-priority coordination messages, real-time search-and-rescue notifications, and Layer 3 offloading signals. The 10% duty cycle and 500 mW maximum power granted to the g3 band by ETSI EN 300 220 provide 10 times longer transmission duration and 20 times higher power capacity compared to the g1 band, thereby ensuring that critical messages are delivered regardless of channel conditions. This two-layer spectrum strategy offers a flexible and scalable response to the variable traffic dynamics of disaster communication, within the ETSI regulatory framework.

2.1.2.8 Parameter Configuration and Dwell Time Analysis

The fundamental bit rate of LoRa is expressed by the following formula:

$$R_b = SF \times \frac{BW}{2^{SF}} \times \frac{4}{4+CR}$$

where BW denotes bandwidth (Hz), SF the spreading factor (7–12), and CR the coding rate (between 4/5 and 4/8). Under ETSI EN 300 220, the maximum duty cycle in the g1 sub-band (868.0–868.6 MHz) is limited to 1%, meaning each node may transmit for a maximum of 36

seconds per hour. In the g3 sub-band (869.4–869.65 MHz), used for high-priority traffic, the duty cycle is 10%, granting 360 seconds of transmission per hour. The dwell time analysis below applies to configurations in the g1 band; 500 kHz BW values correspond to single-channel high-throughput mode. The practical upper limit of 400 ms reflects the operational threshold established in the LoRa Alliance regional parameter table based on US FCC Part 15; the primary regulatory constraint remains the 1% duty cycle under ETSI EN 300 220.

Table 7. LoRa configuration and dwell time compliance analysis

Configuration	Bit Rate (bps)	Theoretical Airtime (ms)	Congested Airtime (ms)	Dwell Limit Compliance
SF7/125kHz	3.418	78,08	96,82	✓ Compliant
SF8 / 125 kHz	1.953	139,78	173,32	✓ Compliant
SF9/125kHz	1.099	246,78	306,01	✓ Compliant
SF10/125kHz	610	493,57	612,02 (exceeds)	✗ Non-compliant
SF7/500kHz	13.672	19,52	24,20	✓ Compliant
SF9/500kHz	4.395	61,70	76,50	✓ Compliant (default)
SF10/500kHz	2.441	123,39	153,01	✓ Compliant
SF11/500kHz	1.343	214,02	265,38	✓ Compliant

At the CR = 4/8 configuration, bit rates decrease by 37.5% compared to CR = 4/5. This reduction shows that while the default SF9/125 kHz configuration (246.78 ms) maintains compliance within the duty cycle budget, SF10/125 kHz (493.57 ms) exceeds the 400 ms dwell limit. For this reason, SF10/500 kHz (123.39 ms) is recommended over SF10/125 kHz when communicating with distant mesh nodes. The 500 kHz BW configurations in the table represent single-channel high-throughput mode; 125 kHz BW is applied for multi-channel frequency diversity. The g3 band (869.4–869.65 MHz, 10% duty cycle) is reserved for time-sensitive traffic and falls outside the scope of this table. The congestion factor (1.24) is derived from literature findings showing that theoretical channel throughput in LoRa networks under a pure ALOHA access model is limited to approximately 18% [11]. This factor reflects the retransmission overhead caused by packet collisions.

2.1.2.9 LoRa Network Capacity and Maximum Number of Served Users

The following capacity calculations are carried out based on a 20-byte packet size anticipated for a typical position/status report in disaster scenarios; while the system supports payloads of up to 242 bytes, short packets utilize the duty cycle budget more efficiently.

The maximum number of users a LoRa node can serve per unit time is calculated by jointly considering the g1 band 1% duty cycle constraint under ETSI EN 300 220, the selected SF/BW configuration, and the Time-on-Air (ToA) parameter. The capacity analysis below is based on the g1 band for routine beacon traffic; time-sensitive high-priority traffic benefits from the 10-times expanded capacity of the g3 band (10% duty cycle).

In the selected SF9/500 kHz configuration, the ToA for a typical 20-byte status/position packet is calculated as approximately 61.70 ms. Under the 1% duty cycle constraint, each node can transmit for a maximum of 36 seconds per hour; accordingly, each node has a capacity of approximately 584 packets per hour.

The literature has shown that the theoretical channel efficiency of LoRa networks under a pure ALOHA access model is limited to approximately 18% [11]. Although using multiple SFs as orthogonal channels increases capacity, inter-SF interference reduces channel utilization [32]. In the proposed three-channel structure (868.1 / 868.3 / 868.5 MHz, each at 125 kHz BW), each channel operates as an independent ALOHA channel; inter-channel interference is minimized through frequency orthogonality. Under the pure ALOHA model, approximately 20 nodes per channel can be supported with a PDR target exceeding 90%, bringing this figure to approximately 60 nodes in the three-channel configuration — a practical capacity increase of 2–2.5× [11, 32]. The theoretical 3× capacity limit represents an upper bound that can be approached under conditions of full channel orthogonality and equal traffic load distribution.

Field studies based on experimental measurements have shown that the maximum number of LoRa nodes capable of operating sustainably in a 1 km² area under a 1% duty cycle condition is limited to 100 [33]. Taking into account data collisions, retransmission overhead, and RF channel saturation, it is recommended that this limit be set more conservatively at 40 nodes/cell. The system's two-tier hierarchical architecture is designed to prevent this limit from being exceeded: when node density in a local cell approaches the threshold, traffic is redirected to Layer 3 via load offloading. Additionally, reserving the g3 band (10% duty cycle, 500 mW) for critical coordination traffic frees the entire g1 band capacity budget for routine beacon traffic, thereby increasing the system's total effective capacity through spectrum layering.

The 40 nodes/cell limit is supported by the pure ALOHA collision model: in the SF9/500 kHz configuration with 20-byte packets, 40 nodes transmitting once per minute generate a load of $G \approx 0.041$ Erlang, and PDR remains at approximately 92%. This value leaves a 15% safety margin for inter-SF interference losses; with the three-channel structure, a total system-level capacity of 120 nodes is reached.

2.1.2.10 LoRa Parameter Configuration

Network performance depends on the interactive optimization of spreading factor (SF), bandwidth (BW), and coding rate (CR) parameters. The parameter set adopted for the proposed disaster communication scenario and the rationale for each selection are summarized in the table below:

Table 8. LoRa parameter configuration and rationale

Parameter	Selected Value	Rationale
Frequency Band	868 MHz (g1: routine) / 869.4–869.65 MHz (g3: critical)	Unlicensed ISM band in Turkey; g3 band provides 10% duty cycle and 500 mW for high-priority traffic
Spreading Factor (SF)	SF9	Optimal balance between range and time-on-air (ToA); SF7–8 insufficient in urban density, SF10+ causes network congestion
Bandwidth (BW)	125 kHz (multi-channel) / 500 kHz (single-channel)	125 kHz: frequency diversity across three channels; 500 kHz: single-channel high-throughput mode

Coding Rate (CR)	4/8	Maximum error correction capability in noisy environments
Duty Cycle	1% (g1, routine traffic) / 10% (g3, critical traffic)	ETSI EN 300 220 g1 and g3 sub-band regulatory compliance
Maximum Payload	242 bytes	Minimizes packet segmentation and time-on-air
RSSI Threshold	–122 dBm	LoRa safe operating lower limit (receiver sensitivity reaches –137 dBm in the SF12/125 kHz configuration)

The literature has shown that the SF9 configuration can achieve a packet delivery ratio (PDR) exceeding 90% under nominal conditions in urban areas; when the number of nodes exceeds 40, PDR has been reported to fall to approximately 65% due to collision effects [13, 33]. This constitutes one of the justifications for the two-tier hierarchical architecture design.

Network routing efficiency is ensured through the ECHO protocol, which is addressed in detail in Section 2.1.2.11 below.

2.1.2.11 Mesh Topology and ECHO Protocol

Unlike the classic LoRaWAN star topology — which is dependent on a central gateway — the proposed architecture adopts a self-healing mesh topology [15, 16]. Each node acts as both an end device and a router; when any node goes offline, data traffic is automatically rerouted through alternative paths.

Network routing is managed through the ECHO protocol. In the Full Flood (FF) phase, a broadcast is sent across the entire network to identify critical nodes and the most efficient paths; in the Pruned Flood (PF) phase, transmissions are sustained only through these critical nodes. This two-phase structure reduces the total number of transmissions across the network by approximately 3 times and decreases per-node energy consumption by more than 50%, according to results reported in the literature [34]. The FF rebroadcast delay is dynamically adjusted according to the selected SF/BW combination and instantaneous traffic load, thereby preserving network currency without exceeding the duty cycle budget.

2.1.2.12 Security and Encryption

In LoRa mesh networks, security constitutes a critical operational requirement in the chaotic RF conditions of disaster environments. Threats such as spoofing, replay attacks, and unauthorized node injection can directly compromise search-and-rescue coordination [35].

In the proposed architecture, these threats are structurally addressed at two separate layers. In the first layer, all command and data traffic between the UAV and the dock station is transmitted over fiber-optic cable, providing hardware-level immunity against RF-based jamming and passive eavesdropping attacks. In the second layer, all over-the-air LoRa mesh communications are protected with AES-128 symmetric block encryption; each node undergoes Pre-Shared Key (PSK) authentication before joining the network [36]. This two-layer security architecture combines the RF immunity advantage of the tethered infrastructure with cryptographic protocols, forming a secure and verifiable communication backbone in the disaster environment.

2.1.3 Layer 3 – High-Altitude Backhaul and Strategic Integration

The upper tier of the two-layer hierarchical architecture provides long-range backbone communication through a high-altitude strategic UAV platform. When the data traffic aggregated by local tethered UAV networks approaches Layer 2 capacity limits, it is redirected to this platform. The sinkhole bottleneck inherent in standard mesh architectures is thereby prevented at the structural level, and network traffic is horizontally balanced. Literature shows that multi-tier non-terrestrial network (NTN) approaches meaningfully extend network lifetime and reliability in disaster scenarios where terrestrial infrastructure has failed [37].

2.2.3.1 Platform Selection and Technical Rationale

The AKSUNGUR High-Payload UAV developed by TUSAŞ is adopted as the reference platform for Layer 3. This selection is the product of a multi-dimensional engineering evaluation based not only on performance criteria, but also on deployability, existing inventory status, and documented operational history in disaster response [19].

AKSUNGUR is a MALE+ class platform supporting a wide mission payload range including satellite communications, radio relay, AIS, PLS, and ELT systems.

Table 9. Critical technical parameters of AKSUNGUR for DTD Layer 3 operation

Parameter	Value	Significance for DTD Architecture
Maximum altitude	40,000 ft (~12,200 m)	LoS coverage over wide geographic area
Payload capacity	750 kg (external)	Supports fully equipped ABS load
Endurance	24 hours (150 kg payload), 50 hours (unloaded)	Long-duration disaster response support
Data link	Dual-redundant, encrypted LOS + SATCOM	Uninterrupted command and control
Radio relay	Integrated (as mission payload)	Layer 2 backhaul interface
Autonomous landing/takeoff	Available	Reduces runway dependency

AKSUNGUR is equipped with a SATCOM system developed by CTech, a TUSAŞ affiliate, enabling beyond-line-of-sight operation with no range constraint other than fuel capacity. This is critical in scenarios where coordination centers are located far from the disaster zone.

2.2.3.2 Offloading Mechanism and Triggering Thresholds

Traffic transfer from Layer 2 to Layer 3 is triggered automatically when any of the following conditions is met. This mechanism is built on a distributed architecture that allows node-level decisions without a central coordinator [38]:

Primary trigger — channel utilization rate: Each Layer 2 UAV node continuously monitors its instantaneous duty cycle usage. When 75% of the total duty cycle budget is consumed, approximately 27 of the 36 available seconds per hour, the node signals offloading mode. This threshold is set to allow intervention before packet collision probability begins to critically degrade PDR [35].

Secondary trigger — queue delay: When the average packet queue delay at a Layer 2 node exceeds 200 ms, offloading is triggered. This value is set to ensure that the system's total end-to-end latency remains below the 300 ms limit prescribed by 3GPP TS 22.179, with the remaining 100 ms margin allocated to transmission and processing delays [39]. Thus, even

when the queue delay trigger threshold is reached, sufficient margin is preserved to keep the system's total latency budget below the standard limit.

Tertiary trigger — node density: When the number of active LoRa nodes in a cell exceeds 35, 87.5% of the 40-node/cell capacity, and neighboring cells also decline to accept additional traffic, traffic is routed directly to Layer 3. This three-level triggering hierarchy avoids burdening Layer 3 with temporary load increases that Layer 2 can handle internally, activating the upper layer only in genuine capacity overflow scenarios.

2.2.3.3 Layer 2–Layer 3 Interface and Protocol Stack

Communication between Layers 2 and 3 runs over an RF-based backhaul link, with two frequency bands functionally separated. Control plane traffic — offloading trigger signals, cell utilization reports, and system management commands — uses a low-bandwidth, high-reliability channel, either the 915 MHz ISM band or AKSUNGUR's encrypted data link system. Data plane traffic — the offloading payload itself — uses the radio relay mission payload aboard AKSUNGUR. Experimental work on two-tier LPWAN architectures confirms that aerial-platform-assisted data channels can provide reliable connectivity even in rural areas [38].

During offload, the Layer 2 node's buffer is flushed and new packet acceptance is paused until the transfer completes — a flow control mechanism that minimizes packet loss during the handover.

2.2.3.4 SATCOM Integration and Beyond-Line-of-Sight Operation

AKSUNGUR's SATCOM infrastructure constitutes the most critical resilience feature of the DTD architecture: the ability for the system to continue operating autonomously even in scenarios where the ground control center is damaged or disconnected. SATCOM integration enables beyond-line-of-sight operation, with no range constraint within the satellite link coverage area. From a system-level perspective, SATCOM integration provides functionality at three levels. At the coordination level, command and control data exchange among AFAD, municipal disaster management centers, and field teams occurs without geographic constraint. At the data aggregation level, survivor location and status data collected from all DTD cells is transmitted via satellite to a centralized evaluation platform. At the redundancy level, if all Layer 2 networks collapse (e.g., cascading tether failure), SATCOM serves as the last-resort communication backbone.

2.2.3.5 Large Platform Constraints and the Complementary Role of the DTD Architecture

The most critical operational constraint of MALE+ class platforms such as AKSUNGUR in disaster communication is runway dependency and preparation time. The platform requires an available airport infrastructure for deployment; in the first critical hours after a disaster, this infrastructure may well be damaged. With 750 kg payload, endurance is approximately 12 hours; unloaded, it reaches 50 hours — meaning the fully equipped ABS configuration significantly reduces mission duration. This constraint explains why the Layer 1–2 components of the DTD architecture are designed as complementary to strategic platforms. Layers 1 and 2, pre-integrated into street lighting poles, can be activated within minutes without human intervention. AKSUNGUR joins the operation hours later, after airspace clearance, and assumes

the long-range backhaul backbone. This time-complementary architecture ensures communication continuity throughout the disaster response.

● 2.3 Population Density-Based Altitude Optimization

2.3.1 Simplification of the Optimization Problem

In the literature, the UAV positioning problem is most commonly formulated as the simultaneous optimization of latitude, longitude, and altitude in three-dimensional space [3]. While this approach is theoretically comprehensive, it carries two practical constraints: its high computational cost makes it difficult to apply in real-time disaster response, and it typically relies on a homogeneous user distribution assumption. In real disaster scenarios, however, individuals cluster at specific gathering points such as schools, parks, and open areas; this multi-modal distribution places a disproportionate burden on network capacity.

In the DTD architecture, the pre-integration of dock stations into urban lighting poles and city infrastructure fundamentally simplifies the problem: the horizontal position (x_dock, y_dock) is fixed at the design stage, reducing the optimization to the determination of the optimal altitude h* along the vertical axis alone. This 3D → 1D transformation not only dramatically reduces computational load, but also allows the actual user density and LoRa capacity constraints to be fully incorporated into the model. The physical validity of this simplification derives directly from the system design constraint: the dock, tether cable, and gravity keep the UAV positioned horizontally above the dock, while altitude can be dynamically controlled by the TMS.

The optimization is carried out in a two-stage hierarchical structure. In the macro-optimization stage, the most suitable dock locations are identified from among candidate urban sites using a user density-based weighted clustering algorithm. In the micro-optimization stage, the optimal altitude that maximizes population-weighted LoS quality is calculated for the fixed dock position. This two-stage structure makes it possible to achieve both reasonable positioning at the global scale and high LoS quality at the local scale simultaneously.

2.3.2 Line-of-Sight Probability and Urban Model

Whether the signal path between the UAV and a ground-level user is obstructed is calculated using a probabilistic line-of-sight (LoS) model based on the statistical distribution of buildings [4]. This model statistically captures the reality that large-scale path loss is affected not only by free-space propagation but also by the surrounding built environment.

The LoS probability as a function of elevation angle (θ, in degrees) is expressed as follows:

$$P_{LoS}(\theta) = \frac{1}{1 + a \cdot exp(-b[\theta - a])}$$

Here, a and b are sigmoid curve coefficients that vary according to the urban morphology of the environment, and are derived based on the building distribution parameters of the ITU-R P.1410-2 standard (α: building coverage ratio, β: building density per unit area, γ: Rayleigh height parameter) [4]. The four environment types defined by ITU-R and their corresponding sigmoid coefficients are presented in Table 10:

Table 10. ITU-R environment types and sigmoid coefficients [2]

Environment Type	α	β (buildings/km²)	γ (m)	a	b
Suburban	0,10	750	8	4,88	0,43
Urban	0,30	500	15	9,61	0,16
Dense Urban	0,50	300	20	12,08	0,11
High-Rise Urban	0,50	300	50	27,23	0,08

With the horizontal distance between the UAV and the i-th user denoted as r_i and UAV altitude as h, the elevation angle is calculated as $\theta_i=\arctan(h/r_i)$ (in degrees). As $P_{LoS}(\theta_i)$ increases, total path loss decreases and link quality improves. With path loss in LoS conditions denoted as PL_{LoS},path loss in NLoS conditions as $PL_{N\,LoS}$, and additional NLoS shadowing loss as η, the expected total path loss is expressed as:

$$PL(\theta, r) = P_{LoS}(\theta) \cdot PL_{LoS} + [1 - P_{LoS}(\theta)] \cdot PL_{N\,LoS}$$

Within this framework, as UAV altitude h increases, θ_i grows, $P_{LoS}(\theta_i)$ ises, and consequently expected path loss decreases. At the same time, however, the UAV–user distance $d_i = \sqrt{h^2 + r_i^2}$increases, causing free-space propagation loss to grow. These two opposing effects make the existence of an optimal altitude h^* mathematically necessary [4].

2.3.3 Capacity Constraint and Duty Cycle Management

In areas of high population density, the duty cycle constraint applied to LoRa's g1 band (1%, ETSI EN 300 220) constitutes a decisive capacity limit for routine beacon traffic [16, 18]. However, since ETSI's g3 sub-band (869.4–869.65 MHz) grants a 10% duty cycle, critical coordination traffic is redirected to this band in situations where high population density causes instantaneous capacity to be exceeded. This constraint limits the transmission duration available to each node within a given time window, reducing collision probability; at the same time, it requires a careful balance between the number of simultaneous users and transmission frequency. In the proposed model, this constraint is integrated into the altitude optimization as follows: in cells with high population density, the duty cycle threshold will be reached more rapidly, necessitating an increase in the number of nodes serving that area and an adjustment of UAV altitude to optimize coverage spread. This multi-constrained optimization approach balances quality of service (QoS) and spectral efficiency jointly. In altitude optimization calculations, the capacity upper bound C_{max} is defined based on the g1 band duty cycle budget. In high-priority scenarios where the g3 band is activated, effective capacity extends beyond this limit; however, this does not affect the routine beacon capacity of g1.

2.3.4 Population Density Function Modeling

The spatial user density λ(x,y) in the disaster area is expressed using a Gaussian Mixture Model (GMM) comprising K gathering points (hotspots) and a background of scattered individuals:

$$\lambda(x,y) = \sum_{k=1}^{K} \frac{N_k}{2\pi\sigma_k^2} exp(-\frac{(x-\mu_{x,k})^2 + (y-\mu_{y,k})^2}{2\sigma_k^2}) + \lambda_{bg}$$

This formulation assumes that the spatial distribution of each gathering area is circularly symmetric (isotropic) and is adequately represented by the standard deviation σ_k. The general GMM extension incorporating a covariance matrix Σ_k for asymmetric clusters may be addressed in future work.

Here, N_k denotes the estimated number of disaster survivors in the k-th gathering area, ($\mu_{x,k}$, $\mu_{y,k}$) the center coordinates of the area, σ_k the spatial spread standard deviation of the cluster, and λ_{bg} the scattered background density of individuals remaining on streets.

Two primary data sources are integrated for the parametric estimation of the λ(x,y) function:

WorldPop Grid: Open-source population density data at 100×100 m resolution provides the pre-disaster baseline distribution. WorldPop data is derived from satellite imagery, settlement maps, and administrative census data using a machine learning–based dasymetric method, and serves as the reference layer for preliminary estimation of user density in disaster areas [40].

Call Detail Records (CDR): CDR data obtained from GSM operators contains real-time cell tower connection records of active devices, mapping post-disaster population movement in near real time. Following the 2015 Nepal earthquake, CDR data from 12 million de-anonymized mobile users was processed within nine days to estimate the spatial and temporal dimensions of population displacement; this approach was shown to provide a viable method for near real-time population mapping in disaster response [41]. The fusion of these two data sources — the spatial completeness of WorldPop and the temporal resolution of CDR — enables reliable estimation of the λ(x,y) function in the disaster area.

Why is the rejection of the homogeneous distribution assumption critical? Standard optimization models [3] assume that users are uniformly distributed across the area. Under this assumption, however, LoRa nodes placed at dense gathering points encounter unexpectedly high traffic loads; the duty cycle constraint is violated far earlier than anticipated, and capacity estimates can deviate significantly from reality. The GMM resolves this problem: each component (k) represents a real gathering point, while the σ_k parameter independently controls the density and spread of clustering at that point.

2.3.5 Derivation of the Normalized Weight Coefficient

The disaster area is divided into N grid cells. For each cell i, the weight coefficient w_i represents that cell's share of total demand in normalized form:

$$w_i = \frac{D_i}{\sum_{j=1}^{N} D_j}, \sum_{i=1}^{N} w_i = 1$$

Where $D_i = \iint_{cell,i} \lambda(x,y)\, dx\, dy$ is the total user demand in the i-th cell. This normalized weighting constitutes an analytical prioritization mechanism that enables the UAV to allocate more resources to high-population areas. In cells where w_i is high and LoS quality deteriorates, the system can undertake proactive interventions such as increasing altitude or offloading traffic to a neighboring node.

2.3.6 Macro-Optimization: Dock Placement (Weighted K-Means)

In the first stage of optimization, the most suitable NN N dock locations are identified from the candidate location set $P_{poles}=\{p_1,p_2,\ldots,p_M\}$ comprising urban lighting poles ($N \ll M$). This is formulated as a Capacitated Facility Location Problem (CFLP).

With the binary decision variable $z_i \in \{0,1\}$ indicating whether a dock is installed at the i-th pole, the objective function maximizes the covered weighted user demand:

$$max\ z_i \sum_{i=1}^{M} z_i \int \int_{A_i} \lambda(x,y)dxdy$$

Subject to the constraints:

$$\sum_{i=1}^{M} z_i \leq N_{drone} \quad (number\ of\ drones)$$

$$\int \int_{A_i} \lambda(x,y)dxdy \leq C_{max} \ \forall i \quad (capacity)$$

$$\int \int_{A_i \cap A_j} \lambda(x,y)dxdy \approx 0 \ \forall i \neq j \quad (coverage\ overlap)$$

When dock locations need to be searched in continuous space, the Weighted K-Means algorithm is applied. Unlike standard K-Means, the centroid update is performed according to the w_i weight of each user, so that docks are placed not merely at geographic centers but at the true center of mass of the population density:

$$min\ J = \sum_{k=1}^{K} \sum_{i \in C_k} w_i \cdot \left|\left|(x_i, y_i) - (x_{D,k}, y_{D,k}\right|\right|^2$$

This problem can be solved using integer linear programming (intlinprog) or greedy heuristic methods.

2.3.7 Micro-Optimization: One-Dimensional Altitude Optimization

In the second stage, the horizontal position (x_{dock},y_{dock}) determined by macro-optimization is fixed, and the problem is reduced solely to the determination of the optimal altitude h^*. This simplification significantly reduces computational cost compared to the 3D positioning problems found in the literature [3], and makes real-time applicability feasible.

Line-of-Sight Probability Model: The probabilistic model of Al-Hourani et al. [4] is used. Within the ITU-R framework, urban morphology is characterized by the building coverage ratio (α), building count per unit area (β), and the mean building height Rayleigh parameter (γ). With the elevation angle between the UAV and the i-th user denoted as $\theta_i = \arctan(h/r_i)$, the LoS probability is calculated as:

$$P_{LoS}(\theta_i) = \frac{1}{1 + a \cdot exp(-b[\theta_i - a])}$$

where a and b are ITU-R constants dependent on urban building density. Example values: for urban environments a≈9.61, b≈0.16; for dense urban a≈12.08, b≈0.11; for suburban a≈4.88, b≈0.43.

Objective Function: The optimal altitude maximizing population-weighted total LoS quality:

$$h^* = arg\ max\ h \sum_{i=1}^{N} w_i \cdot P_{LoS,i}(h)$$

System Constraints:

$$h_{min} \leq h \leq L_{tether}$$

$$\int \int_{A(h)} \lambda(x,y)dxdy \leq C_{max}$$

$$PL(h, R(h)) \leq PL_{max}\ (\approx 136dB)$$

$$F_{Thrust}(h) = (m_{drone} + m_{payload} + m_{tether}(h)) \cdot g + T_{vertical}(h) \leq F_{max}$$

The first constraint defines the physical limit of cable length, the second the LoRa capacity threshold, the third the minimum signal quality, and the fourth the motor thrust limit.

2.3.8 Altitude–Range Trade-off and Autonomous Adaptation Mechanism

While increasing altitude raises LoS probability, it also expands the coverage radius R(h), meaning more users enter the coverage area. However, this simultaneously brings the risk of the duty cycle constraint and capacity limit (C_{max}) being violated more rapidly [16, 18].

Table 11. Optimal elevation angle and altitude ranges by urban morphology

Environment Type	**Optimal θ_{opt}**	**Typical h***	**DTD Compatiblity**
Suburban	~20°	30–50 m	✓ Full
Urban	~42°	60–90 m	✓ Full
Dense Urban	~55–60°	100–150 m	✓ Compatible
High-Rise Urban	>60°	150 m+	⚠ Cable Limit

Taking into account the practical cable length limit of the DTD architecture's tether cable and the load capacity of the UAV motors, the 80–150 m range has been identified as the technically and operationally feasible optimal altitude interval.

The autonomous adaptation mechanism operates through the following loop: the dock station monitors the instantaneous λ(x,y) distribution via Wi-Fi probe requests and CDR updates. When the risk of violating the capacity constraint arises, the system reduces altitude to narrow the coverage radius, with edge users handed over to neighboring UAVs. In the reverse case, when density decreases, altitude is increased to expand coverage. This reactive loop enables the system to continuously adapt to the variable dynamics of the disaster area. **2.4 Autonomous Dock: Operational Safety and Urban Integration**

The autonomous dock station is designed to IP65 protection standards in accordance with the Drone-in-a-Box concept [6]. Visual recognition-based autonomous landing and takeoff management is integrated to enable the UAV to land with centimeter-level accuracy. The dock's power management unit integrates grid power, a backup diesel generator, and solar energy panels within a smart distribution architecture that automatically switches to backup when grid power is lost. All command and telemetry data between the UAV and the dock are transmitted

over fiber-optic cable. This silent backhaul approach makes the system immune to RF jamming attacks, while simultaneously providing full protection against electromagnetic interference from nearby power lines and atmospheric events such as lightning.

2.5 Methodology Summary Table

Component	Design Decision	Role in Design Chain	Source
UAV body	Hexarotor	Stage 2: Platform selection satisfying TWR >= 3 constraint	[9, 10]
Cable structure	Hybrid (Kevlar + G.657A2 + copper)	Stages 2–3: rho_cable, R, mechanical limit definition	[9, 10]
Cable model	Catenary (V_w < 3 m/s) + DAE (V_w > 7 m/s)	Stage 3: m_tether, T_vertical, F_D calculation	[22, 23]
HVDC	48–100 V DC	Stage 5: I^2R minimization, power budget closure	[24]
TWR criterion	>=3.0:1	Stage 4: iterative constraint check	[9]
TMS control	Electromechanical model (load cell + fuzzy logic)	Stages 3–4: tension monitoring analytical basis	[9]
LoRa/Mesh	SF9/125 kHz (multi-channel, frequency diversity) / SF9/500 kHz (single-channel, high-throughput); g1: 868 MHz 1% DC, g3: 869.4–869.65 MHz 10% DC	Stage 6: C_max capacity constraint definition	[11, 12]
ECHO protocol	FF + PF phases	Stage 6: network efficiency optimization	[34]
Wi-Fi access	IEEE 802.11n, dock-based	Stage 1: first-mile hardware solution	[2, 20]
Population model	GMM + WorldPop/CDR	Stage 6: lambda(x,y) and w_i computation	[40, 41]
Macro-optimization	Weighted K-Means / CFLP	Stage 6: dock placement decision	[1, 5]
Micro-optimization	1D Al-Hourani LoS	Stage 6: h* determination within capacity + thrust constraint context	[1, 2]
Network architecture	Two-tier hierarchical mesh	All stages: sinkhole prevention, scalability	[15, 16, 37]

Table 12. dtd architecture design decisions, role in design chain, and sources

3. RESULT

The proposed Dock–Tether–Drone (DTD) architecture was developed as an integrated synthesis of free-flying UAV-based communication systems, tethered aerial platforms, and multi-tier mesh network approaches found in the literature. System performance is evaluated here along four dimensions — network coverage and reliability, energy continuity, first-mile access, and system resilience — and linked to the outputs of the methodological stages. Each performance evaluation is a direct reflection of the models established and the design constraints defined in the methodology section.

3.1 Network Coverage and Reliability Performance

In the DTD architecture, network coverage performance is significantly improved compared to classical UAV-based systems thanks to the multi-layer communication structure. The ground station-based IEEE 802.11n access layer offers a stable connection range of 200–250 m in open-area conditions, while providing better penetration capability compared to the 5 GHz band in debris and multipath fading environments. This result validates the 802.11n selection decision justified in Section 2.2.1.At the LoRa layer, the SF9/500 kHz single-channel configuration with a ToA of 61.70 ms is fully compliant with the ETSI g1 band 1% duty cycle constraint. Assuming one transmission per minute for routine beacon traffic, duty cycle utilization remains at 0.1%; critical coordination traffic benefits from the 10-times expanded transmission capacity of the g3 band (10% duty cycle, 500 mW). In open-area conditions, the three-channel structure (868.1/868.3/868.5 MHz, each at 125 kHz BW) can accommodate close to 120 nodes without exceeding the 75% threshold of the g1 duty cycle budget. In high-density scenarios where this threshold is exceeded, the system activates the g3 band to ensure delivery of critical messages. This capacity value is a direct output of the analytical capacity model established in Section 2.2.2.9.The ECHO protocol's two-phase FF+PF structure reduces the total number of transmissions across the network by approximately 3 times and decreases per-node energy consumption by more than 50% [34]. These gains not only improve energy efficiency but also increase the channel's potential load-bearing capacity: the reduction in transmission count directly decreases spectral collisions, improving PDR performance. These results are consistent with the experimental findings of Saraereh et al. [13], who report significantly higher PDR in UAV-assisted LoRa networks compared to ground-based systems.

3.2 Energy Continuity: The Contribution of the Tethered Architecture

From an energy continuity perspective, the tethered structure represents the architecture's most decisive advantage. In free-flying UAV systems, operational duration is constrained to 25–40 minutes depending on battery capacity; the DTD architecture transcends this limitation by relocating the energy source to the ground station.

The HVDC critical voltage analysis (Equations (4) and (5)) shows that at an operating condition of $U/U_0 \geq 2$, transmission losses remain at approximately 7% of the payload power. When compared to the 50% loss at $U/U_0 = 1$, the effect of voltage ratio optimization on system efficiency is clearly evident. Equation (6) analyticstructure represents the architecture's most decisive advantage. In free-flying UAV systems, operational duration is constrained to 25–40 minutes depending on battery capacity; the DTD architecture transcends this limitation by relocating the energy source to the ground station.The HVDC critical voltage analysis (Equations (4) and (5)) shows that at an operating condition of $U/U_0 \geq 2$, transmission losses remain at approximately 7% of the payload power. When compared to the 50% loss at $U/U_0 = 1$, the effect of voltage ratio optimization on system efficiency is clearly evident. Equation (6) analytically demonstrates that the minimum power requirement scales linearly with drone mass, confirming that minimizing cable mass is decisive not only aerodynamically but also for energy efficiency.Nonetheless, the mass and aerodynamic drag added by the cable to the system increases thrust requirements. Within the framework of Equation (7), at 100 m cable length, cable mass (1.55 kg) and the vertical component of cable drag increase the total thrust requirement, directly affecting the TWR margin. The TWR $\geq$ 3:1 constraint (Table 5) incorporates the safety margin needed to absorb this effect. Therefore, the energy continuity advantage is a holistic system output that must be evaluated in conjunction with power supply and thrust design.

3.3 First-Mile Problem and Wi-Fi-Based Access Solution

The first-mile problem describes the difficulty disaster survivors face in establishing initial connectivity to the communication network. Two root causes are documented in the literature: high path loss when attempting direct connection to a high-altitude aerial platform [2], and insufficient antenna power of end devices under variable RF conditions [20].

The DTD architecture resolves this problem at the hardware level. User data is collected at the ground-level dock station via IEEE 802.11n and then transmitted to the UAV through the G.657A2 fiber-optic line within the tether. This approach yields two concrete outcomes. First, the user device connects only to a ground access point within a range of 200–250 m; thus, both path loss and antenna power requirements remain at manageable levels. Second, since the user connection is transferred from the RF channel to the fiber-optic channel, interference and signal shadowing caused by the chaotic RF environment of the disaster area no longer affect connection quality.

The selection of the fiber-optic line in accordance with the G.657A2 standard forms the physical basis of this solution: data transmission is maintained with attenuation of ≤0.21 dB/km even at a minimum bend radius of 7.5 mm, ensuring compatibility with the small drum radius encountered during autonomous takeoff and landing cycles. The rationale for this selection is presented in detail in Section 2.2.2.2.

3.4 Two-Tier Mesh Architecture and Sinkhole Mitigation

In standard single-layer mesh architectures, network traffic tends to concentrate as it approaches the exit points (gateways); this leads to a traffic accumulation phenomenon known as the sinkhole bottleneck, in which the nodes closest to the central gateway are disproportionately burdened [15, 16]. The proposed two-layer hierarchical structure resolves this issue at the architectural level.

In the LoRa mesh network at Layer 2, traffic load is distributed through the Pruned Flood mechanism of the ECHO protocol: only critical nodes are retained in the transmission chain, while all other nodes are exempted from load forwarding. When Layer 2 capacity approaches its limit — defined as 75% of the duty cycle budget or queue delay exceeding 200 ms (set to leave a 100 ms margin relative to the 300 ms end-to-end latency target of 3GPP TS 22.179) — traffic is offloaded to Layer 3; this offloading mechanism ensures that the Layer 2 network remains within its optimal working region.

This hierarchical structure is directly consistent with the findings of Ozturk et al. [46], which report that multi-layer NTN approaches significantly increase network lifetime in disaster scenarios. Deriving the offloading trigger thresholds from the capacity analysis of Malik et al. [45] places this consistency on a solid analytical foundation.

3.5 Comparative Assessment: Tethered vs. Free-Flying Systems

Compared to free-flying UAV systems, the DTD architecture's primary advantages center on energy continuity, predictable position stability, and an interference-resistant communication backbone. Battery constraints in free-flying systems determine flight duration, platform cost, and operational logistics simultaneously. The tethered structure removes this variable.

Operational constraints of tethered systems should not be overlooked, however. The 150 m cable length limit constrains both altitude and maneuverability. In narrow, complex urban environments — dense building clusters, high-voltage lines, bridge underpasses — cable management creates operational difficulties where free-flying systems are clearly superior. The DTD architecture acknowledges this trade-off explicitly and positions tethered UAVs as the preferred solution for sustained, fixed-position disaster communication missions.

3.6 System Resilience Under Stress Conditions

Resilience is analyzed under three stress scenarios.

High wind conditions (V_w > 7 m/s): The model selection rule automatically shifts to the lumped-mass DAE model; cable tension is computed segment by segment and managed through TMS active tension control. The TWR ≥ 3:1 criterion incorporates sufficient margin to absorb the 15–20% propeller interference loss and up to 60% power increase from VRS risk.

Power supply interruption: Upon grid loss, the dock's smart power management unit switches to backup (battery/diesel) within ≤50 ms — a duration too short to threaten UAV hover stability. The MAVLink Failsafe protocol detects power loss and transitions the UAV to internal battery mode, initiating safe landing [9].

Network node failure: The self-healing property of the mesh topology automatically reroutes traffic through alternative paths when any node goes offline. Because the ECHO protocol's FF phase periodically rediscovers critical nodes, adaptation delay to topology changes remains bounded.

3.7 Limitations

Despite its strengths, the system has several technical limitations. Cable length and weight directly constrain UAV maximum altitude and maneuverability, creating operational difficulties in narrow and complex urban environments. LoRa's low data rate and duty cycle limitations pose a bottleneck for high-volume data applications. Urban integration of dock stations involves physical installation, electrical connection, and permitting processes that carry practical operational challenges.

The scope of this work is conceptual, mathematical, and analytical design validation. Simulation environments and physical prototype construction are outside its scope; field-experimental verification is identified as a primary research objective for future studies. All models are grounded in sources validated through field or simulation work, but the consistency of these models with integrated system behavior under this specific architectural configuration remains an open research question.

3.8 Comparison with the Literature and Practical Applicability

While most existing works treat coverage optimization and energy efficiency as separate problems, this study addresses them within a single architectural framework — a characteristic that distinguishes it from the dominant approach in the literature. Data capacity is relatively limited compared to high-bandwidth solutions, but low infrastructure dependency, rapid deployability, and energy autonomy make this trade-off acceptable in a disaster management context.

From a practical standpoint, the proposed system offers a feasible solution for AFAD and municipal disaster management units, as well as search-and-rescue coordination centers. Pre-deploying dock stations at strategic urban reference points — schools, parks, municipal buildings — and integrating them with mobile UAV systems can create a communication infrastructure that activates without human intervention at the moment of disaster. The modular structure also allows straightforward adaptation across different disaster scales, from neighborhood to district level.

4. CONCLUSION

This study proposed a Dock–Tether–Drone (DTD) architecture designed to address the communication vulnerabilities that emerge when critical infrastructure collapses during disasters. The limited operational duration of UAV-assisted networks, first-mile signal attenuation, and network sinkhole bottlenecks were treated not as isolated problems but as interconnected challenges addressed simultaneously within a functional decomposition framework.

The architecture's core contribution operates at three levels. At the first level, the performance ceiling imposed by the conventional approach of integrating energy generation and data transmission on a single aerial platform is eliminated by assigning each function to an independently optimizable physical layer. At the second level, the first-mile problem is resolved at the hardware level through a ground-level Wi-Fi access point that collects user data and a fiber-optic cable that carries it to the UAV. At the third level, sinkhole congestion is addressed architecturally through a two-tier hierarchical mesh structure with analytically justified offloading thresholds.

Every design decision in the methodology is grounded in a physical constraint, an operational safety threshold, or an analytic model — from cable length limits and LoRa configuration selection to TWR criteria and HVDC voltage ratios. The design chain is coherent by construction rather than by coincidence.

4.1 Future Work

Field validation is the most immediate priority. The current work remains at the level of analytic modeling and architectural design; controlled field tests across different urban morphologies (dense urban fabric, industrial zones, rural areas) will experimentally verify the coverage, reliability, and latency values the system can deliver in practice.

Integration of higher-capacity communication layers is another critical research direction. LoRa's low data rate and duty cycle constraints limit the system for bandwidth-intensive applications. Adding 5G NR-U or Wi-Fi 6E as an additional communication layer could address data-intensive disaster response needs such as video streaming and high-resolution map sharing.

Artificial intelligence–assisted network and traffic management stands out as a research area that can significantly enhance the adaptability and efficiency of the system. Deep reinforcement learning–based algorithms can optimize UAV altitude based on real-time user density data, distribute traffic load evenly across nodes, and perform proactive rerouting by predicting network failures. This approach will enable the system to adapt in real time to the unpredictable dynamics of disaster conditions.

Multi-drone coordination and swarm intelligence is also worth investigating. Since a single tethered UAV's coverage area is physically limited, architectures in which multiple dock-drone pairs operate in coordination could expand coverage while improving resilience against single-point failures.

Finally, advances in **tether cable technology** warrant ongoing attention. Lighter, higher-voltage-capacity composite cable materials and active cable stabilization mechanisms could extend the system's operational flexibility in complex urban environments.

REFERENCES

[1] Indu, C., &Vipin, K. (2024). 3D deployment of multi-UAV network in disasterzonestoachievecoverageandconnectivity. *2024 International Conference on CognitiveRoboticsandIntelligentSystems (ICC-ROBINS)*.

[2] Al-Hourani, A., Kandeepan, S., &Lardner, S. (2014). Optimal LAP altitudeformaximumcoverage. *IEEE Wireless Communications Letters, 3*(6), 569-572.

[3] McRae, J. N., Nielsen, B. M., Gay, C. J., Hunt, A. P., &Nigh, A. D. (2021). Utilizingdronesto restore andmaintainradiocommunicationduringsearchandrescueoperations. *Wilderness&EnvironmentalMedicine, 32*(1), 41-46.

[4] Janssen, T., BniLam, N., Aernouts, M., Berkvens, R., &Weyn, M. (2020). LoRa 2.4 GHz communication link andrange. *Sensors, 20*(11), 3066.

[5] PueyoCentelles, R., Freitag, F., Meseguer, R., Navarro, L., Ochoa, S. F., & Santos, R. M. (2019). A LoRa-basedcommunicationsystemforcoordinatedresponse in an earthquakeaftermath. *Proceedings of the 16th International Conference on Information SystemsforCrisisResponseand Management (ISCRAM)*.

[6] Zang, Z., Ma, J., Li, C., Wang, H., Jing, R., &Shi, Y. (2024). A design of automatic UAV dock platform system. *AppliedSciences, 14*(1), 456.

[7] Qiu, W., Shao, X., Masui, H., &Liu, W. (2024). Optimizing droneenergyuseforemergencycommunications in disastersviadeepreinforcementlearning. *Future Internet, 16*(245).

[8] Zeng, Y., & Zhang, R. (2017). Energy-efficient UAV communicationwithtrajectoryoptimization. *IEEE Transactions on Wireless Communications, 16*(5), 2747-2760.

[9] Fattori, F., &Cocuzza, S. (2025). Tethereddrones: A comprehensivereview of technologies, challenges, andapplications. *Drones, 9*(425).

[10] Marques, M. N., Magalhães, S. A., Dos Santos, F. N., &Mendonça, H. S. (2023). Tetheredunmannedaerialvehicles: A systematicreview. *Robotics, 12*(117).

[11] Bor, M., Vidler, J., &Roedig, U. (2016). LoRaforthe Internet of Things. *Proceedings of the 2016 International Conference on Embedded Wireless Systemsand Networks (EWSN)*, 361-366.

[12] Cattani, M., Boano, C. A., &Römer, K. (2017). An experimentalevaluation of thereliability of LoRalong-rangelow-powerwirelesscommunication. *Journal of Sensor andActuator Networks, 6*(2), 7.

[13] Saraereh, O. A., Alsaraira, A., Khan, I., &Uthansakul, P. (2020). Performanceevaluation of UAV-enabledLoRanetworksfordisastermanagementapplications. *Sensors, 20*(8), 2156.

[14] Meshtastic Project. (2024). Meshtastic documentation: LoRa configuration. https://meshtastic.org/docs/configuration/radio/lora/

[15] Syed, D. S., Hossain, S. B., Islam, A., Jim, T.-A.-I., &Zishan, M. S. R. (2024). Design andfeasibilityanalysis of a LoRabasedcommunicationsystemfordisastermanagement. *AIUB Journal of ScienceandEngineering, 23*(2).

[16] Yen, C. X., Shanmugam, K., & Rana, M. E. (2023). Short-term mobile ad hoc network withLoRabasedinfrastructure in disasterrelief. *(Akademik Bildiri/Yayın)*.

[17] Li, L., Zhu, L., Huang, F., Wang, D., Li, X., Wu, T., & He, Y. (2024). Post-disasteremergencycommunicationsenhancedbydronesandnon-orthogonal multiple access: Three-dimensionaldeploymentoptimizationandspectrumallocation. *Drones, 8*(63).

[20] Darwajkar, A., Hendre, G., Bhiware, S., & Mali, A. S. (2020). Drone-basedno-internet communication network. *International Journal of Advanced Research in Science, CommunicationandTechnology (IJARSCT)*.

[21] He, W., & Zhang, S. (2022). Stability parameter range of a tethered unmanned aerial vehicle. *Shock and Vibration, 2022*, Makale 4893721. https://doi.org/10.1155/2022/4893721

[22] Koenemann, J., Williams, P., Sieberling, S., & Diehl, M. (2017). Modeling of an airborne wind energy system with a flexible tether model for the optimization of landing trajectories. *IFAC-PapersOnLine, 50*(1), 11944–11950.

[23]Beffert, M., & Zell, A. (2026). *Real-time quasi-static modeling of UAV tether aerodynamics* (arXiv:2512.22588v2). arXiv. https://doi.org/10.48550/arXiv.2512.22588

[24] Socol, Y. (2026). High voltage DC power transmission for tethered UAV systems. *(TechRxiv preprint.)* https://doi.org/10.36227/techrxiv.175693715.53817256/v2

[25] Faishal, A., Setyadewi, I. T., Aklis, N., Harjanto, F., Wibowo, A. M., & Supriyanto, A. (2025). Comparative study of propeller thrust force on unmanned aerial vehicle using ground testing methods and theoretical calculations. *Engineering Proceedings, 84*(1). https://doi.org/10.3390/engproc2025084059

[26]Šćuric, A., Krznar, N., Penđer, A., Štedul, I., & Kotarski, D. (2025). Autonomous multirotor UAV docking and charging: A comprehensive review of systems, mechanisms, and emerging technologies. *Symmetry, 17*(11), Makale 1988. https://doi.org/10.3390/sym17111988

[27] Heydarnia, O., Wauters, J., Lefebvre, T., & Crevecoeur, G. (2024). *An optimal control framework for airborne wind energy systems with a flexible tether* (arXiv:2407.14258). arXiv. https://doi.org/10.48550/arXiv.2407.14258

[28] Fagiano, L. (2017). Systems of tethered multicopters: Modeling and control design. *IFAC-PapersOnLine, 50*(1), 4706–4711. https://doi.org/10.1016/j.ifacol.2017.08.919

[29] Petäjäjärvi, J., Mikhaylov, K., Pettissalo, M., Janhunen, J., & Iinatti, J. (2017). Performance of a low-power wide-area network based on LoRa technology: Doppler robustness, scalability, and coverage. *International Journal of Distributed Sensor Networks, 13*(3). https://doi.org/10.1177/1550147717699412

[30] Semtech. (2015). *SX1276/77/78/79 datasheet*, Rev. 4. Semtech Corporation.

[31] Meshtastic Project. (2024). *LoRa configuration*. Meshtastic Documentation. https://meshtastic.org/docs/configuration/radio/lora/

[32] Georgiou, O., & Raza, U. (2017). Low power wide area network analysis: Can LoRa scale? *IEEE Wireless Communications Letters, 6*(2), 162–165. https://doi.org/10.1109/LWC.2016.2647247

[33] Malik, M., Kothari, A., & Pandhare, R. (2024). Scalability analysis of LoRa and Sigfox in congested environment and calculation of optimum number of nodes. *Sensors, 24*(20), Makale 6673. https://doi.org/10.3390/s24206673

[34] Hasson, M., Chakareski, J., & Yapici, Y. (2024). Flooding in LoRa mesh networks. *2024 IEEE International Conference on Communications (ICC)*, 1–6. https://doi.org/10.1109/ICC51166.2024.10622567

[35] Aras, E., Ramachandran, G. S., Lawrence, P., & Hughes, D. (2017). Exploring the security vulnerabilities of LoRa. *2017 3rd IEEE International Conference on Cybernetics (CYBCONF)*, 1–6. https://doi.org/10.1109/CYBConf.2017.7985777

[36] Tsai, K. L., Huang, Y. L., Leu, F. Y., You, I., Huang, Y. L., & Tsai, C. H. (2018). AES-128 based secure low power communication for LoRaWAN IoT environments. *IEEE Access, 6*, 45325–45334. https://doi.org/10.1109/ACCESS.2018.2852563

[37] Ozturk, M., Ciloglu, B., Koc, G. B., & Yanikomeroglu, H. (2024). *Multi-tier non-terrestrial networking for disaster communications: A layered clustering approach* (arXiv:2404.15229). arXiv. https://doi.org/10.48550/arXiv.2404.15229

[38] Sobot, S., Lukic, M., Bortnik, D., Nikic, V., Lima, B., Beko, M., & Vukobratovic, D. (2023). *Two-tier UAV-based low power wide area networks: A testbed and experimentation study* (arXiv:2305.11267). arXiv. https://doi.org/10.48550/arXiv.2305.11267

[39] 3rd Generation Partnership Project. (2016). *Technical Specification Group Services and System Aspects; Mission Critical Push To Talk (MCPTT) over LTE; Stage 1 (Release 13)* (3GPP TS 22.179 V13.3.0). https://www.3gpp.org/ftp/Specs/archive/22_series/22.179/22179-d30.zip

[40] WorldPop Project. (2018). *Global high resolution population denominators project*. School of Geography and Environmental Science, University of Southampton; CIESIN, Columbia University. https://www.worldpop.org

[41] Wilson, R., zu Erbach-Schoenberg, E., Albert, M., Power, D., Tudge, S., Gonzalez, M., Guthrie, S., & Bengtsson, L. (2016). Rapid and near real-time assessments of population displacement using mobile phone data following disasters: The 2015 Nepal earthquake. *PLOS Currents Disasters, 1*. https://doi.org/10.1371/currents.dis.d073fbece328e4c39087bc086d694b5c

MEDIA SOURCES

[18] Yeni Şafak (2023). Afet bölgesinde iletişim sıkıntısı çeken vatandaşlardan Turkcell'e: Uçan baz istasyonlarınız nerede? Erişim Adresi: https://www.yenisafak.com/gundem/afet-bolgesinde-iletisim-sikintisi-ceken-vatandaslardan-turkcelle-ucan-baz-istasyonlariniz-nerede-4505771

[19] DefenceTurk (2023). AKSUNGUR İHA'dan deprem bölgeleri için iletişim desteği! Erişim Adresi: https://www.defenceturk.net/aksungur-ihadan-deprem-bolgeleri-icin-iletisim-destegi

[38] DefenceTurk (2023). AKSUNGUR İHA'dan deprem bölgeleri için iletişim desteği! Erişim Adresi: https://www.defenceturk.net/aksungur-ihadan-deprem-bolgeleri-icin-iletisim-destegi